Mälardalen University

This is an accepted version of a paper published in *Fire safety journal*. This paper has been peer-reviewed but does not include the final publisher proof-corrections or journal pagination.

Citation for the published paper:
Hansen, R., Ingason, H. (2011)
"An Engineering tool to calculate heat release rates of multiple objects in underground structures"
Fire safety journal, 46(4): 194-203
URL: http://dx.doi.org/10.1016/j.firesaf.2011.02.001

Access to the published version may require subscription.

Permanent link to this version:
http://urn.kb.se/resolve?urn=urn:nbn:se:mdh:diva-11304

http://mdh.diva-portal.org

An Engineering tool to calculate heat release rates of multiple objects in underground structures

Rickard Hansen[1]
Haukur Ingason[1,2]

[1]Mälardalen University
Box 833
721 23 Västerås
Sweden

[2]SP Technical Research Institute of Sweden
Box 857
501 15 Borås
Sweden

Abstract

Simple theoretical calculations of the overall heat release rate (HRR) of multiple objects have been carried out. The results were compared to fire experiments in a model tunnel using wood cribs placed at equal distance from each other. Three different methods are presented which are based on physical relations for fire spread between the wood cribs. The first method uses a critical heat flux as ignition criteria while the other two methods use an ignition temperature. The method using the critical heat flux as ignition criteria shows very good agreement with the corresponding experimental results used. The two methods using the ignition temperature as ignition criteria did not agree well with the corresponding experimental results. The prerequisites, that the methods should be kept relatively simple to be of practical use and that the burning objects should not necessarily have to be of uniform composition, were fulfilled.

Notation

c_p =specific heat (kJ/kg·K)
F =view factor
h =lumped heat loss coefficient (kW/m^2·K)
h_c =convective heat loss coefficient (kW/m^2·K)
h_r =radiative heat loss coefficient (kW/m^2·K)
h_t =total heat loss coefficient (kW/m^2·K)
k =thermal conductivity (W/m·K)
k_s =time width coefficient
$L_{f,calc}$ =calculated flame length (m)
$L_{f,obs}$ =observed flame length (m)
$\dot{m}_a$ = mass flow (kg/s)

n_s =retard index
P =perimeter of tunnel (m)
p =total number of piles
$\dot{q}''_{cr}$ = critical heat flux (kW/m^2)
$\dot{q}''_{flux}$ = external heat flux (kW/m^2)
$\dot{q}''_{\max}$ = maximum heat release rate per unit area (kW/m^2)
$\dot{Q}$ = heat release rate (HRR) (kW)
$\dot{Q}_{\max}$ = maximum HRR (kW)
r_s =amplitude coefficient
s =pile number in a sequence of piles
t =time (s)
T_a =ambient temperature (K)
T_{avg} =average gas temperature (K)
T_f =average temperature at the fire (K)
T_g =gas temperature (K)
T_s =surface temperature (K)
ΔT_f =average excess temperature at the fire location (K)
ΔT_{ft} =excess temperature rise at the flame tip (K)
x =location of interest (m)
α =thermal diffusivity (m^2/s)
ε =emissivity factor
σ =Stefan-Boltzmann constant, $5.67 \cdot 10^{-11}$ kW/m^2·K^4

Introduction

The HRR of a HGV (Heavy Goods Vehicle) cargo can play an essential role with respect to fire hazard in a tunnel or in an underground mine. A cargo with potentially high energy content may by far be the dominating factor when describing the fire behaviour of a vehicle. The various types of cargos transporting on roads makes it difficult to find a common design fire. As the HRRs of a single or multiple HGVs may vary, an engineering tool for estimating the HRR would be quite useful for fire protection engineers. This may apply also for other professionals working with fire protection of underground constructions.

This article describes a potential engineering tool to calculate the HRR of multiple objects. The model basically sums up the individual HRR curves from each object by estimate when ignition between objects occurs. The HRR for each object is represented by an exponential function of time. In the case when the HRR to be predicted pertains to a single HGV, consisting of a cargo with for example piled wood pallets, the model can predict the heat release of the entire fire load based on information of one pile of wooden pallets, whereas if there is a risk of fire spread between multiple HGVs it can predict the total heat release of the convoy. The exponential curves used originate from the work by Numajiri and Furukawa [1]. Ingason [2] [3] has further developed the concept and introduced the design parameters: maximum HRR ($\dot{Q}_{\max}$), total energy content (E_{tot}) and the retard index (n), which is an arbitrarily chosen parameter with no physical meaning. Based on these parameters the time to maximum HRR ($t_{\max}$) and the fire duration (t_d) can be calculated. Other parameters that are used in the model include the amplitude coefficient (r) and the time width coefficient (k), which are calculated based on the information given.

The method assumes that HRR curve is known *a priori* from experiments for parts of the fire load or for a single HGV fire load in the case of a convoy. Describing the HRR curves mathematically with a single exponential expression makes the design process possible. In real life all ignition of the adjacent items may not be known beforehand. Therefore the method needs to be improved, involving physical models to determine the time of ignition of adjacent items.

In order to improve the methodology, three different models were tested. The first model uses a critical heat flux as ignition criteria and the other two methods use an ignition temperature. These three models can for example be used when designing a HRR curve for a HGV cargo.

In order to validate the proposed engineering tool, a comparison with experimental data has been used. The experimental data was obtained from model scale experiments presented by Ingason [4] that were performed to investigate fire spread between adjacent vehicles in tunnels. These tests were found to be very well defined and fit very well to the aim of the work presented here. The vehicles were simulated using wood cribs and the distance between the wood cribs was constant. This made it possible to make the necessary comparison.

In the following, the model scale tests presented by Ingason [4] are outlined together with the theories for the models used to predict the fire spread.

Model scale fire experiments

In the report by Ingason [4] a series of tests in a model tunnel are presented. A total of 12 tests were carried out in a 1:23 scale model tunnel. The use of scale modelling is very convenient as it allows us to translate the results from model scale fire experiments into a full scale system. The scale modelling technique uses the theory of dimensionless groups as a basis. As the model tunnel in the fire experiments was built in scale 1:23 it means that the size of the tunnel was scaled geometrically according to this ratio. Neglecting the influence of the thermal inertia of the involved material, the turbulence intensity and radiation, but scaling the HRR, the time, flow rates, the energy content and mass, we end up with scaling models found in Table 1.

Table 1. List of scaling models [4].

Unit	Scaling model	Equation number
Heat release rate [kW]	$\dot{Q}_F = \dot{Q}_M \cdot \left(\frac{L_F}{L_M}\right)^{5/2}$	(1)
Velocity [m/s]	$u_F = u_M \cdot \left(\frac{L_F}{L_M}\right)^{1/2}$	(2)
Time [s]	$t_F = t_M \cdot \left(\frac{L_F}{L_M}\right)^{1/2}$	(3)
Energy [kJ]	$E_F = E_M \cdot \left(\frac{L_F}{L_M}\right)^{3} \cdot \frac{\Delta H_{c,M}}{\Delta H_{c,F}}$	(4)
Mass [kg]	$m_F = m_M \cdot \left(\frac{L_F}{L_M}\right)^{3}$	(5)
Temperature [K]	$T_F = T_M$	(6)

In Table 1, L is the length scale, the index F relates to the full scale and the index M relates to the model scale. Thus in our actual model F is 23 and M is 1.

Regarding the similarity between model scale and full scale experiments, there is a relatively well defined similarity between model scale and full scale. Although it is impossible and not necessary to preserve all the terms obtained by scaling theory simultaneously in model scale tests, the terms that are most important and most related to the study are preserved. The thermal inertia of the involved material, turbulence intensity and radiation are not explicitly scaled, and the uncertainty due to the scaling is difficult to estimate. However, the Froude scaling has been used widely in enclosure fires and results from model scale tests seems fit full scale well, see references [5-10]. Since the ratio of tunnel length to tunnel height should be large enough to scale a realistic tunnel fire, it is very expensive to build a model tunnel in a full scale. In our opinion, the scaling ratio should not be smaller than approximately 1:20 in order to preserve the Froude number and to avoid producing a laminar flow in the model tunnel. Our experience of model tunnel fire tests in this scale shows there is a good agreement between model scale and full scale on many focused issues [11-15]. Such kind of scale is widely used in model tunnel fire tests all over the world [16-19].
The parameters that were varied during the experiments were: the number of wood cribs, type of wood cribs, the longitudinal ventilation rate and the ceiling height. The tests were carried

out with longitudinal ventilation under different fire conditions. Longitudinal ventilation was established using an electrical axial fan attached to the entrance of the model tunnel, see Figure 1. Longitudinal wind velocities of 0.42 m/s, 0.52 m/s,
0.62 m/s and 1.04 m/s were used in the test series. The effect of different ventilation rates on the fire growth rate, fire spread, flame length, gas temperatures, radiation and smoke backlayering, was investigated.

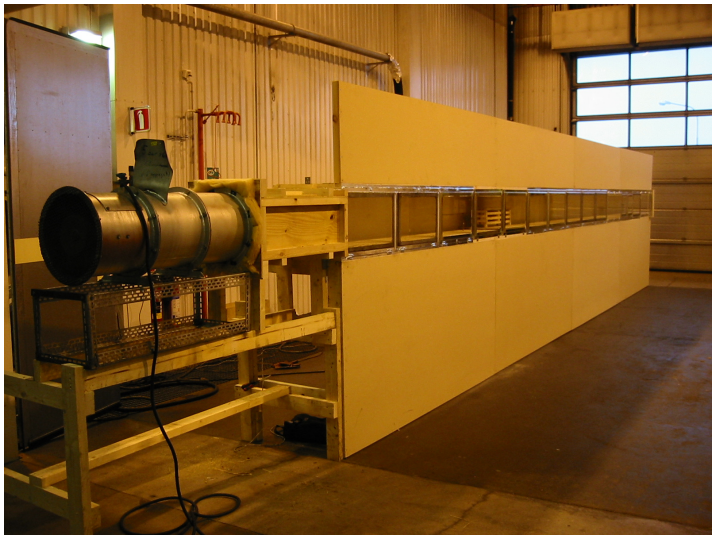

Figure 1. A photo of the model scale tunnel.

The tunnel itself was 10 m long, 0.4 m wide and tests were performed using two different heights: 0.2 m and 0.3 m, respectively. Wood cribs were used to simulate the fire source, which was designed to correspond to a scaled down HGV fire load. The fire load consisted of varying numbers of wood cribs (pine). The mass of the wood cribs varied from test fire to test fire. Each wood crib corresponded to a large scale mass – using equation (5) - of approximately 27 ton, thus representing an HGV load. The variation in mass was due to the fact that each wood crib was manufactured by hand. The free distance between each horizontal stick was 0.019 m and the total fuel surface area of wood crib was estimated to be 0.90 m^2, see Figure 2.

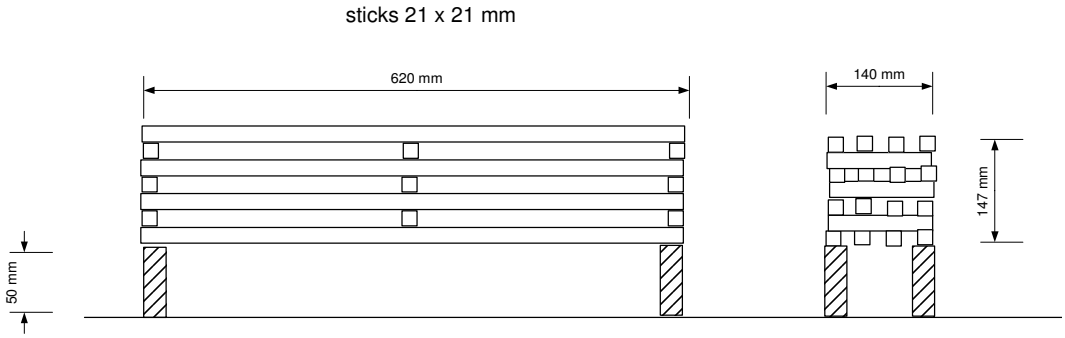

Figure 2. Detailed drawing of the large wood cribs.

The wood cribs used in each test were dried overnight in a furnace at 60 ºC (<5% moisture). The first wood crib was placed on the weighing platform at a height 50 mm above floor level. A cube of fibreboard measuring 0.03 m × 0.03 m × 0.024 m, which was soaked in heptane (9

mL) was placed on the weighing platform board at the upstream edge of the wood crib. At 2 minutes from start of the logging system, this cube was ignited. Additional wood cribs were placed downstream of the first wood crib. These additional cribs were not weighed. A schematic of the experimental setup is given in Figure 3.

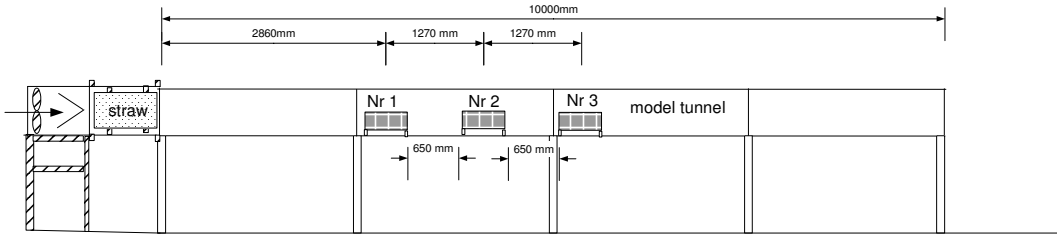

Figure 3. Locations of the fuel load with three wood cribs arranged in series.

Full details of all tests conducted are summarised in reference 4. Tests 1, 3 and 4 were chosen for closer examination and comparison to modelling. The reasons for choosing test 1, 3 and 4 were that they were conducted with one, two and three wood cribs respectively, the same height of the tunnel was used, the same type of wood crib was used in the experiments and that the wood cribs in test 3 and 4 were placed in serie. Table 2contains a summary of the input data of the three tests.

Table 2. Summary of test 1, 3 and 4 by Ingason [4].

Test nr	**T_a (C)**	**Nominal longitudinal centreline velocity (m/s)**	**Number of wood cribs used**	**Weight of each wood crib (kg)**	**Maximum total energy content (MJ)**	**Distance between wood cribs (m)**
1	20.0	0.64	1	2.292	37.7	-
3	18.9	0.62	2	2.296; 2.210	74.1	0.65
4	18.6	0.62	3	2.298; 2.412; 2.336	115.9	0.65

The dimensions of the tunnel were 0.4 m (W) × 0.3 m (H). The height between the top of wood crib and ceiling was in all three cases 0.1 m. As seen from the input data above, the three test fires were conducted under similar conditions. The only difference is that test number 1 was conducted with one wood crib while tests 3 and 4 were conducted with two and three wood cribs respectively. Therefore the result of test number 1 can be used to compare the HRR curve of a single item and the results of tests 3 and 4 can be used to compare the HRR curve for multiple objects. The nominal longitudinal centreline velocity in all three cases was relatively low, which is desirable as the issue of a tilting flame does not have to be accounted for in the methods described here. The ideal situation would be to obtain test results performed during zero longitudinal centreline velocity but such results were not available. The low ceiling of the model tunnel will lead to that the flame is deflected at the ceiling level. But as the flame length is not used in the heat transfer calculations – instead the gas temperature is used when calculating the radiative heat transfer – this issue is not addressed.

The HRR curves were obtained for the three fire tests [4] are given in Figure 4. The method of determining the HRR is described in the report by Ingason [4].

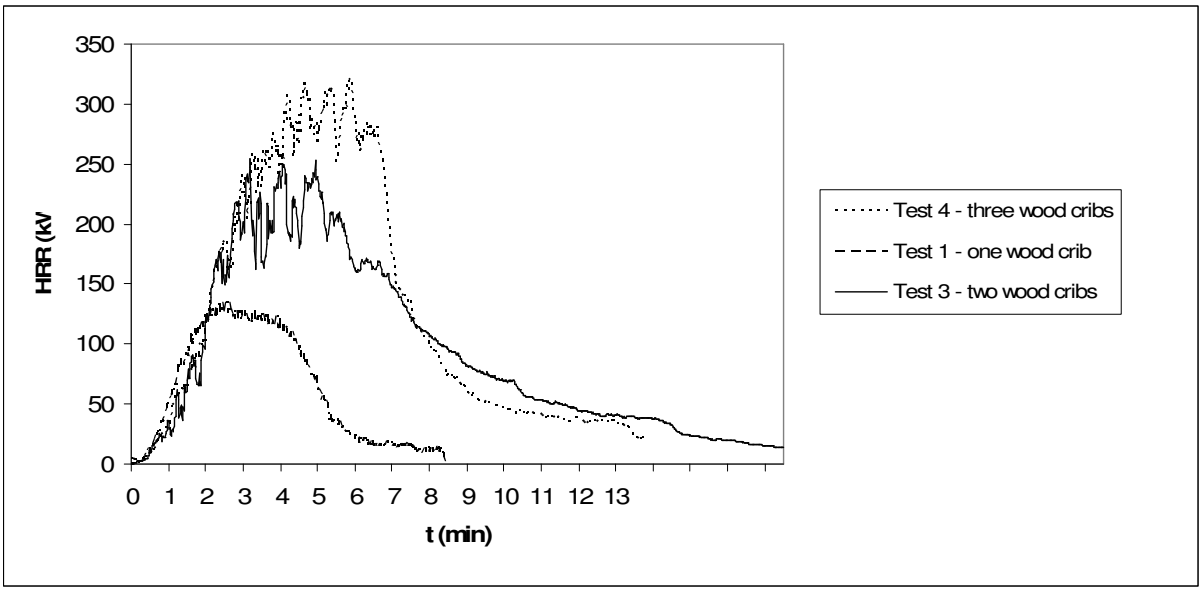

Figure 4. The HRR for fire test number 1 with one wood crib, fire test number 3 with two wood cribs and fire test number 4 with three wood cribs.

Table 3 lists the mass flow rate inside the tunnel, the maximum HRR and the maximum total heat flux for the three tests. Max flux 1 was measured 0.885 m (=3·H) downstream of the fire, max flux 2 was measured 3.36 m (=11.2·H) downstream (at the second wood crib) and max flux 3 was measured 5.855 m (=19.5·H) downstream (at the third wood crib).

Table 3. The mass flow, maximum HRR and maximum total heat flux of the three test fires by Ingason [4].

Test fire	$\dot{m}_a$ **(kg/s)**	$\dot{Q}_{\max}$ **(kW)**	**Max flux 1 (kW/m^2)**	**Max flux 2 (kW/m^2)**	**Max flux 3 (kW/m^2)**
1	0.077	135.3	-	4.0	1.4
3	0.065	254.7	61.0	33.4	11.5
4	0.066	320.8	60.5	83.5	18.0

The maximum average temperatures for the three test fires are found in Table 4, the maximum average temperatures were calculated from the measured maximum values from a set of five thermocouples placed at various heights, 3.36 m downstream of the first wood crib.

Table 4. The maximum average temperatures of fire test 1, 3 and 4 by Ingason [4].

Test fire	**$T_{avg,\,max}$ (°C)**
1	309.3
3	639.3
4	906.0

Method using summation of objects HRRs

Ingason [2] proposed a method to estimate the HRR given as a single exponential function of time instead of several functions for different time intervals, see Figure 5. The work of Ingason is based on the work by Numajiri and Furukawa [1] and is only applicable to fuel controlled fires, or fires with a small or negligible constant maximum HRR period. The method assumes uniform conditions – simplifying the input data. The design parameters are the peak HRR ($\dot{Q}_{\max}$), the total calorific value, E_{tot} and the retard index (n), which is an arbitrarily chosen parameter with no physical meaning. Based on these parameters, the time to the peak HRR ($t_{\max}$) and the fire duration (t_d) can be calculated. Other parameters used in the model include the amplitude coefficient (r) and the time width coefficient (k), which are calculated based on the input parameters the peak HRR and the total calorific value. The main challenge with the method is to relate the retard index n to some physically identifiable number.

When designing a HRR curve where several objects are included, the retard index governs when the HRR curve of each object starts to develop (the higher n , later the start), i.e. when the fire exits the incipient phase. Thus, the method implicitly includes the incipient phase (the time from ignition until the fire growth rate starts to be significant). The time difference when the fire spreads from one object to another is not constant. Indeed this difference tends to shorten as the fire spread from the first object to the second etc. For every object, a value of n is adjusted during curve fitting (applying the least squares fit technique), so the incipient phase is exited approximately when it is expected that the fire will spread to that specific object. The method is based upon the assumption that the parameter n_s increases linearly, as uniform conditions are a prerequisite when using this method, for example: n_1=1, n_2=3, n_3=5, n_4=7 etc. As a result of this assumption the time to ignition of the individual cargo items (objects) will not vary linearly.

When designing a HRR curve where several objects are included, the initial work will focus on the measured HRR curve of the initial object, applying curve fitting to obtain a suitable value of n . The appearance of the resulting HRR curve will be dictated by the linear increase of n in combination with the total calorific value (E_{tot}) and the peak HRR ($\dot{Q}_{\max}$) of each object. The total time interval can be used as an aid when estimating the difference in n . The method is suitable for HGV cargo where the cargo items are placed in close proximity to each other (for example stacked cardboard boxes, pallets etc.). The method could is also suitable for use when, e.g., reconstructing an actual fire.

The concept of using information from a single burning item (object) to predict – by summation – the total history of HRR is not a new; see for example Wickström and Göransson [20]. What is new here is the treatment of the mathematical expression for the single burning item.

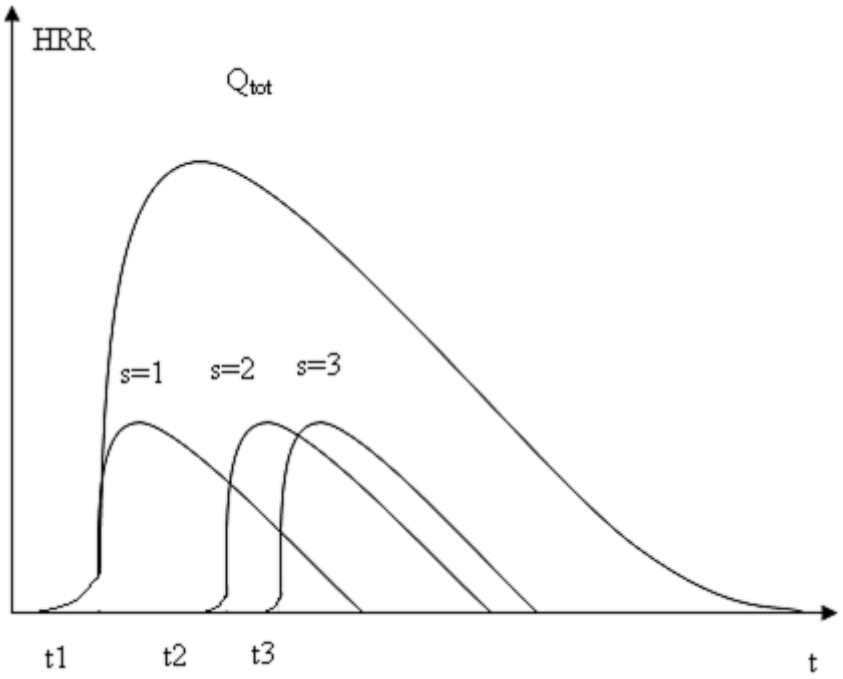

Figure 5. The summation of individual HRR curves adding to a total HRR curve. The figure displays the ignition time of the individual items (objects). As noted the ignition of the adjacent item will vary non-linearly.

The method uses the following equation when calculating the sum of all individual HRR:

$$\dot{Q} = \sum_{s=1}^{p} \dot{Q}_{\max,s} \cdot n_s \cdot r_s \cdot (1 - e^{-k_s \cdot t})^{n_s - 1} \cdot e^{-k_s \cdot t} \qquad \text{[kW]} \qquad (7)$$

Where:

p is the total number of objects

s is the pile number in a sequence of objects

$\dot{Q}_{\max,s}$ is the maximum HRR [kW]

t is time [s]

n_s is a retard index

r_s is an amplitude coefficient

k_s is the time width coefficient

The amplitude coefficient and the time width coefficient are calculated for each type of object using the following equations:

$$r_s = \left(1 - \frac{1}{n_s}\right)^{1-n_s} \qquad (8)$$

$$k_s = \frac{\dot{Q}_{\max,s}}{E_{tot,s}} \cdot r_s \qquad (9)$$

$$t_{\max,s} = \frac{\ln(n_s)}{k_s} \tag{10}$$

Applying the least squares fit technique to fire tests 1, 3 and 4 using a spreadsheet gives the result shown in Figure 6.

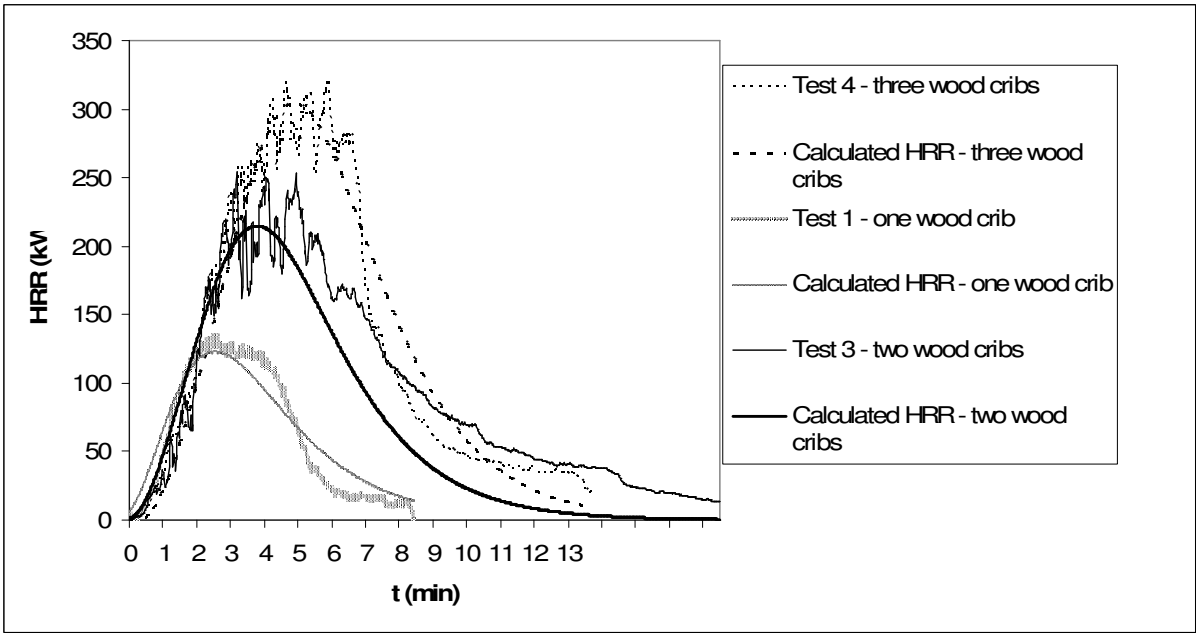

Figure 6. The measured HRR and the calculated HRR of fire test number 1, 3 and 4.

The calculated HRR was fitted to the measured HRR (applying the least squares fit technique), using a different retard index for each of the three test fires. The indices used are summarised in Table 5.

Table 5. Index and coefficients of the three test fires with $\dot{Q}_{\max} = 0.1353$ *MW for wood crib 1.*

	Test fire #1	Test fire #3	Test fire #4
n_1	5.2	5.2	5.2
n_2		12.2	12.2
n_3			19.2
r_1	2.22	2.22	2.22
r_2		2.22	2.22
r_3			2.22
k_1	0.00859	0.00859	0.00859
k_2		0.00859	0.00859
k_3			0.00859

These indices resulted in the following expression for the first test fire:

$$\dot{Q}_{calculated,\,fire\#1} = 0.1353 \cdot 5.2 \cdot 2.22 \cdot (1 - e^{-0.00859 \cdot t})^{4.2} \cdot e^{-0.00859 \cdot t} \tag{11}$$

The difference in increase of n for each object (dn) was found to be best fitted by 7 using the least squares fit technique. This difference is an indication of the time delay between the ignitions of the three wood cribs.

As can be seen from the HRR curves in Figure 6, the rate of rise of the calculated HRR curves increases at the ignition of the second and third wood crib, respectively. This is due to the fact that the ignitions of the adjacent wood cribs take place before the peak value of the total HRR curve, thereby increasing the steepness of the curve.

Possible methods using physical relationships

The method assumes that the HRR curve of the first single object is known *a priori* from experiments. By adjusting only the n parameter it is possible to reconstruct the HRR for double and triple sets of adjacent wood cribs, respectively. The physical ignition phenomena are included in the mathematical treatment by summing up two or three identical fire curves. In real life all HRR curves may not be known *a priori* and conditions cannot always be assumed to be uniform. Thus the method must be improved, involving physical models to determine the time of ignition of adjacent items.

The following three methods, involving more physics, do not rely solely on summing up single fire curves as the previous method and do not assume uniform conditions.
The three methods are based upon a relatively straightforward algorithm and a spreadsheet can be used to expedite the calculations.

In order to further validate the results of the three methods, the energy content of the resulting heat release curves is calculated and compared with the actual energy content. Furthermore, the calculated ignition times of the adjacent wood cribs were used to compare the results of the three methods with that presented previously based on summation of object HRRs. The retard index values and HRR curves for the different methods were then compared. In order to quantify the time when the fire exits the incipient phase it was assumed that the incipient phase is exited when $\frac{\Delta \dot{Q}}{\Delta t} \geq 0.2$, i.e. when the rate of rise of the HRR curve starts to be significant.

Method using external critical heat flux as ignition criteria

As we are dealing with a fire with a transient external heat flux, methods assuming a constant external heat flux cannot be used. This applies, for example, to the method of Tewarson [21] where an ignition time, t_{ig} , is calculated using a constant external heat flux and a thermal response parameter and a critical heat flux value of the material. When determining the time of ignition, the following relationship from Ingason [4] was used for determining the external heat flux:

$$\dot{q}''_{flux} = h_c(T_{avg} - T_a) + F \cdot \varepsilon \cdot \sigma(T_{avg}^4 - T_a^4) \qquad [\text{kW/m}^2] \qquad (14)$$

Where:

h_c is the convective heat loss coefficient, which is set to 0.005 kW/m^2·K (in accordance with what was reported by Ingason [4])
T_{avg} is the average gas temperature [K]
T_a is the ambient temperature [K], which is set to 293 K for fire test number 1, 3 and 4, even though T_a was 291.9 K and 291.6 K for fire test number 3 and 4 respectively
F is the view factor, which is set to 1 (in accordance with Ingason [4])
ε is the emissivity factor, which is set to 0.8 (in accordance with Ingason [4])
σ is the Stefan-Boltzmann constant, 5.67·10^{-11} kW/m^2·K^4

Ignition occurs when:

$$\dot{q}''_{flux} = \dot{q}''_{cr} \qquad (15)$$

The critical external heat flux value for wood, $\dot{q}''_{cr}$, is assumed to be 13.1 kW/m^2 (Monterey Pine with a moisture content of 0 %), Babrauskas [22].

In Figure 7, the total heat flux was plotted using equation (14) and the measured values from the performed fire experiments. The experimental data fit the measured data by Ingason [4] very well.

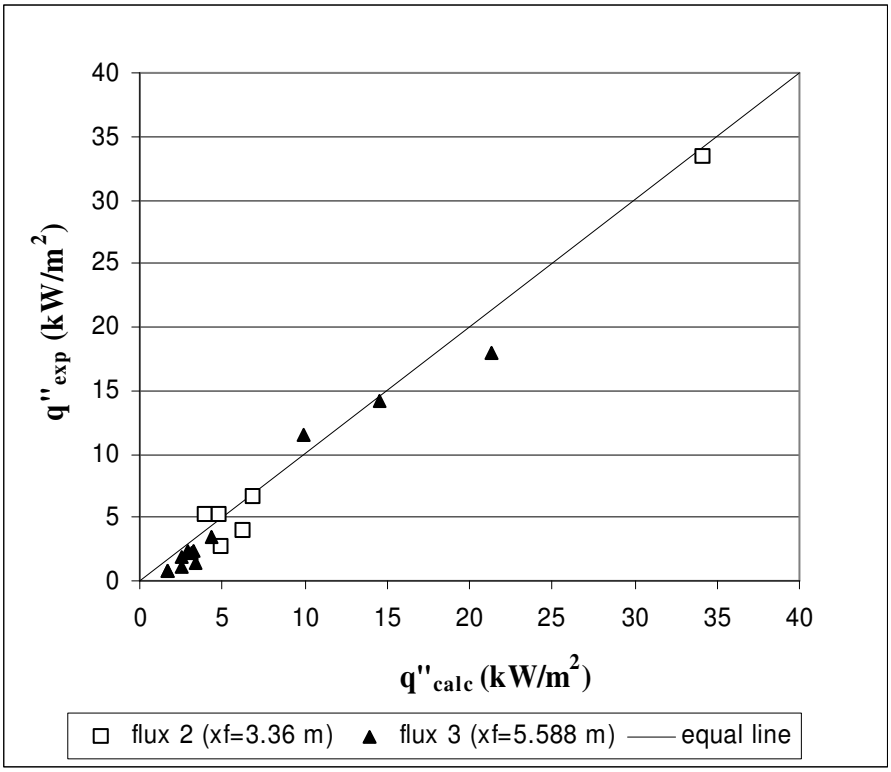

Figure 7. The measured total heat flux as a function of the calculated heat flux using equation (14) from Ingason [4].

The average gas temperature, T_{avg}, is calculated using the following expression from Ingason [4]:

$$\frac{\Delta T_{avg}(x)}{\Delta T_f} = e^{\left(\frac{-hPx}{\dot{m}_a c_p}\right)} \qquad (16)$$

Where:
$\Delta T_f = (T_f - T_a)$ is the average excess temperature at the fire location [K]
h is the lumped heat loss coefficient, which is set to 0.016 kW/m^{2}K for the stack closest to the fire and 0.023 kW/m^{2}K for the stack furthest to the fire (in accordance with Ingason [4]).
P is the perimeter of the tunnel [m]
x is the location of interest [m]
$\dot{m}_a$ is the massflow [kg/s]
c_p was set to 1.0 kJ/kg·K

The average temperature at the fire, T_f, is calculated using the following expression from Ingason [4]:

$$T_f = T_a + \frac{2}{3}\frac{\dot{Q}}{\dot{m}_a c_p} \qquad (17)$$

The HRR of the first wood crib is calculated using equation (11) developed for test fire number 1. The fire is assumed to be fuel controlled (no lack of oxygen in the vicinity of the fire source).

Based on calculated values for T_f and T_{avg}, the external heat flux, $\dot{q}''_{flux}$, at the wood crib closest to the fire could be calculated.

Using the calculated external heat flux, ignition of the second wood crib, which is closest to the first wood crib, was found to occur after 88 seconds assuming $\dot{q}''_{flux}$ >13.1 kW/m^2. The HRR of the second wood crib was therefore added to the HRR of the first wood crib, starting at t_2=88 seconds by adjusting the value of n_2 so it would correspond to $t = t_{i,2} = 88$ seconds.

A comparison between the calculated HRR curve and the measured values of the test fire involving two wood cribs is shown in Figure 8:

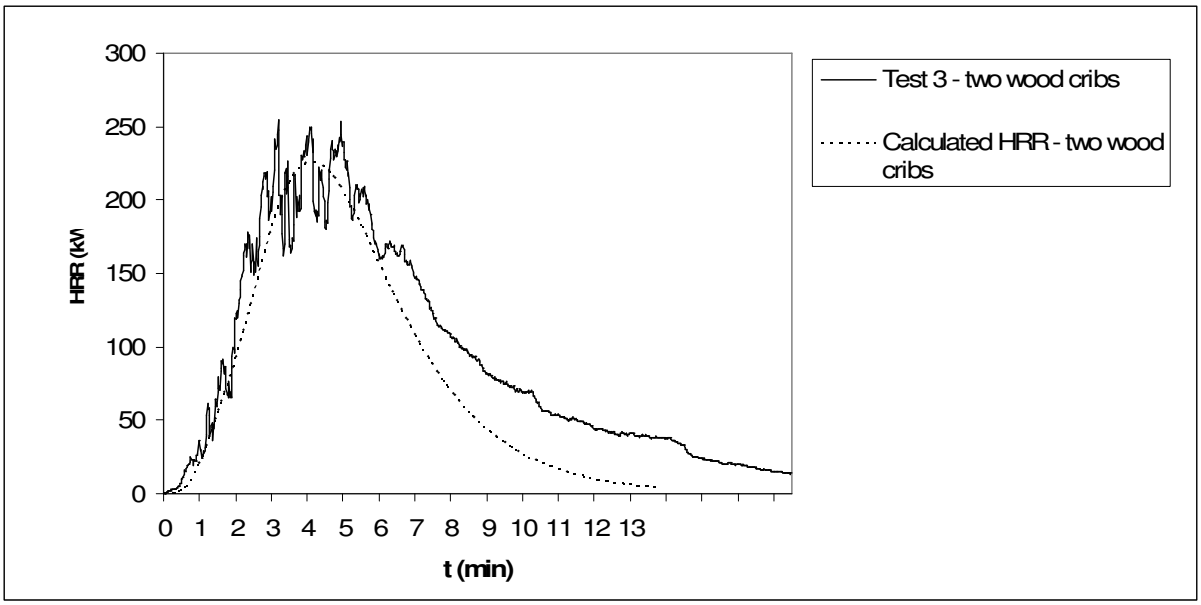

Figure 8. The HRR using the method with the critical heat flux as ignition criteria versus the measured HRR value.

As seen in Figure 8, the method agrees very well with the measured values of test fire #3.

The external heat flux at the third wood crib is calculated using the same method as previously. Ignition of the third wood crib was found to occur after 126 seconds. A comparison between the calculated HRR curve and the measured values of the test fire involving three wood cribs is given in Figure 9.

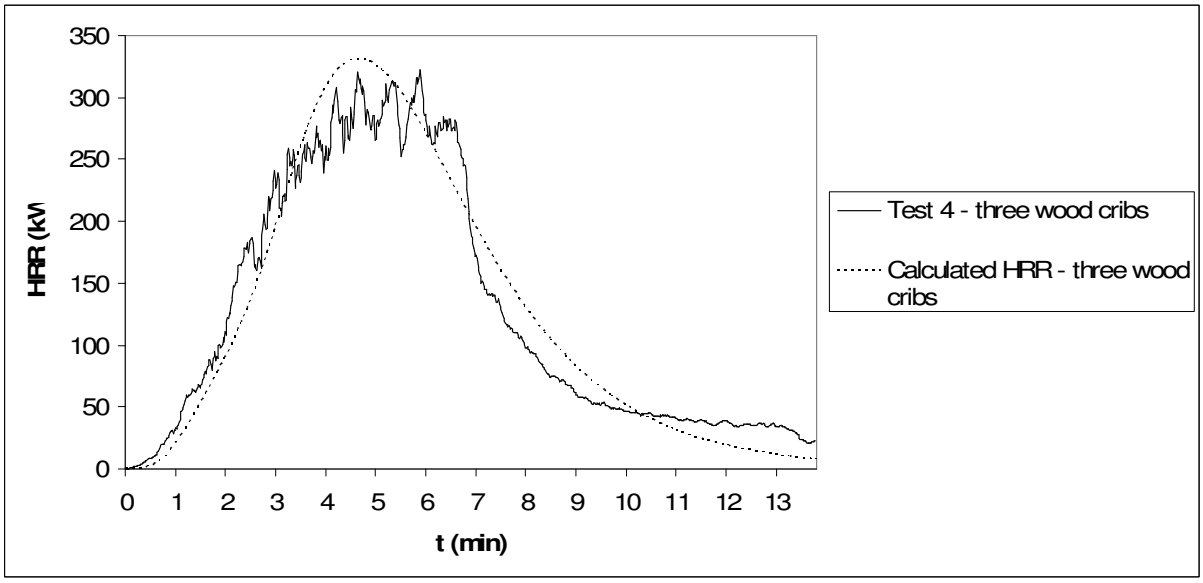

Figure 9. The HRR using the method with the critical heat flux as ignition criteria versus the measured HRR value.

As seen in Figure 9, the method agrees very well with the measured values from test 4.

The method with the critical heat flux as ignition criteria resulted in the following expressions for the HRR:

$$\dot{Q} = 0.1353 \cdot 5.2 \cdot 2.22 \cdot (1 - e^{-0.00859 \cdot t})^{4.2} \cdot e^{-0.00859 \cdot t} \quad , t < 89 \qquad (18)$$

$$\dot{Q} = 0.1353 \cdot 5.2 \cdot 2.22 \cdot (1 - e^{-0.00859 \cdot t})^{4.2} \cdot e^{-0.00859 \cdot t} + 0.1353 \cdot 5.2 \cdot 2.22 \cdot (1 - e^{-0.00859 \cdot (t-88)})^{4.2} \cdot e^{-0.00859 \cdot (t-88)}$$

$$, t \leq 126 \qquad (19)$$

$$\dot{Q} = 0.1353 \cdot 5.2 \cdot 2.22 \cdot (1 - e^{-0.00859 \cdot t})^{4.2} \cdot e^{-0.00859 \cdot t} + 0.1353 \cdot 5.2 \cdot 2.22 \cdot (1 - e^{-0.00859 \cdot (t-88)})^{4.2} \cdot e^{-0.00859 \cdot (t-88)} + 0.1353 \cdot 5.2 \cdot 2.22 \cdot (1 - e^{-0.00859 \cdot (t-126)})^{4.2} \cdot e^{-0.00859 \cdot (t-126)} \qquad (20)$$

In order to further verify the results of the method as the total calorific value is a parameter part of the method, the total energy content of the calculated HRR curve and the energy content based upon the total mass of the involved wood cribs (i.e. the actual energy content) were compared. These results are summarised in Table 6. One conclusion based on the comparison is that the two methods for calculation of the energy content matches well.

Table 6 Energy content calculated based on HRR curve or total mass.

Test #	Energy content based on HRR curve (MJ)	Energy content based on total mass (MJ)
3	70,0	74,1
4	105,0	113,4

Using the calculated ignition time of the second wood crib (88 seconds) and the third wood crib (126 seconds), the following retard index values were determined: $n_1 = 5.1$, $n_2 = 10.5$, and $n_3 = 15.1$. These values resulted in the heat release curves shown in Figure 10.

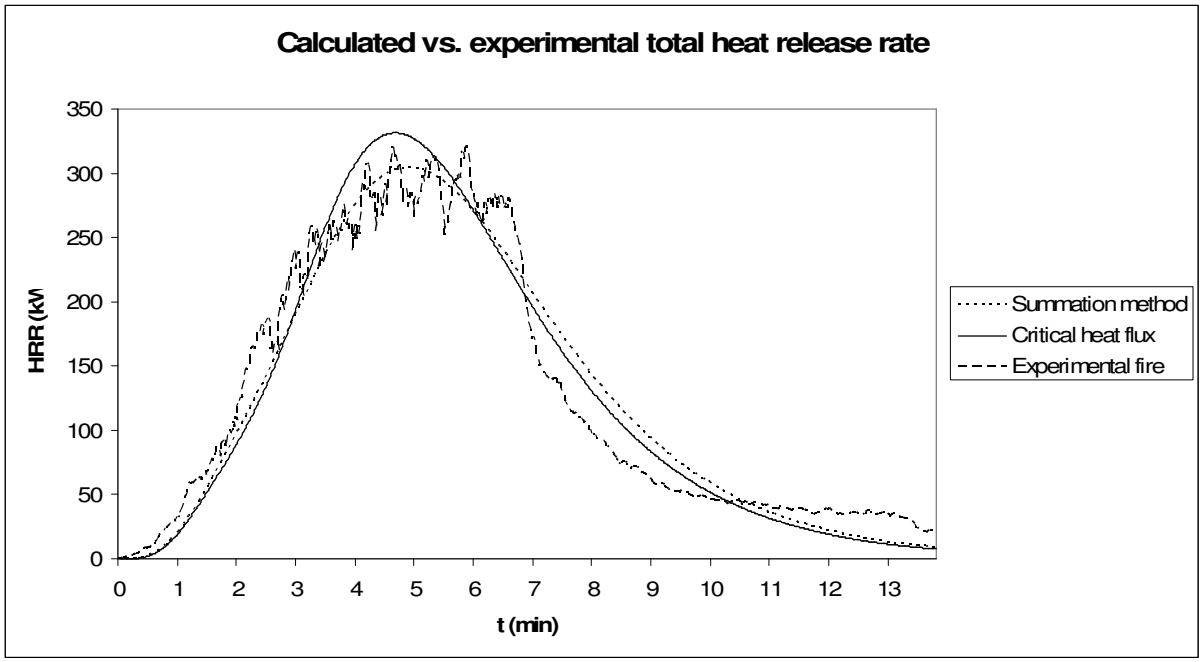

Figure 10. The calculated total HRR curve of the summation method and the method using the critical heat flux as critical value.

When comparing the retard index values and the total HRR values with the values from the method using summation of objects HRRs, it is clear that a consistent value of *dn* can be

established from the figures above (i.e. $dn \approx 5$). Also the two calculated HRR curves are very similar.
Performing a sensitivity analysis of the retard index values with respect to the criterion regarding the exit of the incipient phase ($\frac{\Delta \dot{Q}}{\Delta t} \geq 0.2$). The criterion was changed to 0.1 and 0.3 respectively. The resulting retard index values for the two cases were: n_2=10.4 and n_3=15 in the case of $\frac{\Delta \dot{Q}}{\Delta t} \geq 0.1$; n_2=10.6 and n_3=15.2 in the case of $\frac{\Delta \dot{Q}}{\Delta t} \geq 0.3$. Thus a conclusion here is that the criterion is not very sensitive to changes and will only result in minor changes in the corresponding retard index values.

Two methods using ignition temperature as ignition criteria

Refining the physical method described in the section above could, for example, include using an ignition temperature instead of a critical heat flux, in order to account for the heat progressively accumulated at the surface of the wood crib. When calculating the surface temperature of the wood crib, both convection and radiation boundary conditions should be accounted for. This would most likely better account for any time delay to ignition after the critical heat flux has been reached, which the previous method does not take into account. Further, using an ignition temperature instead of a critical heat flux enables us to take into account the fact that we are actually dealing with a transient heat flux and not a constant heat flux (an increasing surface temperature will reflect the increasing heat flux).

As most equations for calculation of the surface temperature assume a constant heat flux, a numerical method was used when solving the equations listed below. Assuming a thermally thick material, the following equation from Holman [23] was used when calculating the surface temperature:

$$-k \frac{\partial T}{\partial x}\Big]_{x=0} = h_t \left(T_g - T_s\right) \qquad (21)$$

Where:
T_g is the gas temperature [K]
h_t is the total heat loss coefficient [W/m²·K]
T_s is the surface temperature [K]
k is the thermal conductivity [W/m·K]

The value T_g above was assumed to be equal to T_{avg} and calculated using the same procedure as in the earlier method, i.e.:

$$h_t = h_c + h_r \qquad (22)$$

Where:
h_c is the convective heat loss coefficient [W/m²·K] and is set to 5 W/m²·K (in accordance with Ingason [4]).
h_r is the radiative heat loss coefficient [W/m²·K]

$$h_r = \varepsilon \cdot \sigma \cdot (T_g + T_s) \cdot (T_g^2 + T_s^2) \quad (23)$$

Applying a numerical method (finite-difference) when solving the expression above, simplifies the procedure to a two-dimensional heat transfer problem. The finite-difference approximation for a surface node is given by:

$$T_{m,n}^{i+1} = \tau \cdot \left(2 \cdot T_g^i \cdot \frac{h_t \cdot \Delta x}{k} + 2 \cdot T_{m+1,n}^i + T_{m,n+1}^i + T_{m,n-1}^i + \left(\frac{1}{\tau} - 2 \cdot \frac{h_t \cdot \Delta x}{k} - 4 \right) \cdot T_{m,n}^i \right) \quad (24)$$

Where:

$$\tau = \frac{\alpha \cdot \Delta t}{(\Delta x)^2} \quad (25)$$

Where:
α is the thermal diffusivity [m^2/s]
Δt is the time increment [s]
Δx is the distance increment [m]

The thermal diffusivity is given by:

$$\alpha = \frac{\lambda}{\rho \cdot c_p} \quad (26)$$

Where:
λ is the thermal conductivity [W/m·K]

The finite-difference approximation for an internal node is given by:

$$T_{m,n}^{i+1} = \tau \cdot \left(T_{m+1,n}^i + T_{m-1,n}^i + T_{m,n+1}^i + T_{m,n-1}^i \right) + (1 - 4 \cdot \tau) \cdot T_{m,n}^i \quad (27)$$

The finite-difference approximation for a corner node is given by:

$$T_{m,n}^i = 2 \cdot \tau \cdot (T_{m+1,n}^i + T_{m,n+1}^i - 2 \cdot T_{m,n}^i + 2 \cdot \frac{h_t \cdot \Delta x}{k} \cdot (T_g^i - T_{m,n}^i)) + T_{m,n}^i \quad (28)$$

The following value was found for pine (Monterey Pine with a moisture content of 0%) [22]:

- Ignition temperature: 622 K
- Density: 460 kg/m³

The following value was found for pine (moisture content of 0%) [22]:

- Heat capacity: 1.8 kJ/kg·K
- Thermal conductivity: 0.185 W/m·K

Thus the thermal diffusivity is calculated:

$$\alpha = \frac{0.185}{460 \cdot 1800} \approx 2.23 \cdot 10^{-7} \text{ m²/s}$$

It was further assumed that the emissivity factor is 1 and the fire was fuel controlled fire. To ensure convergence, the time increment (Δt) was set to 0.1 s and the distance increment (Δx) was set to 0.0005 m. Using the T_{avg} values calculated previously, results in the following curve for the corner node temperature at the second wood crib using a spreadsheet:

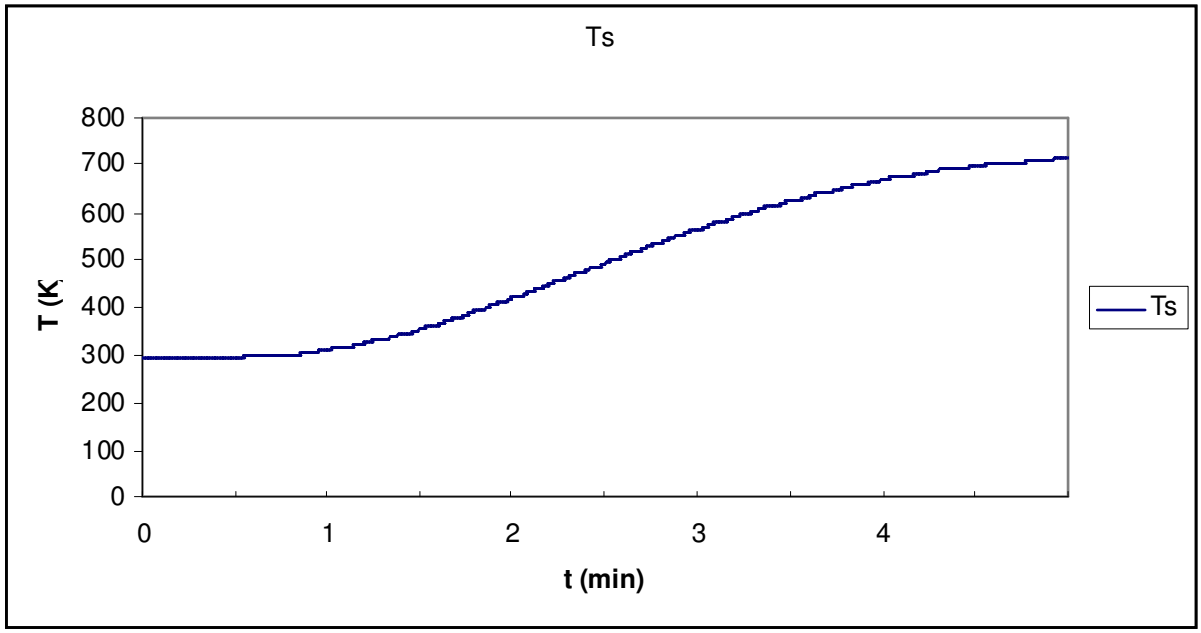

Figure 11. The corner node temperature at the second wood crib as a function of time.

The surface temperature was found to exceed the ignition temperature at 622 K after ~208 seconds at the corner nodes. The HRR of the second wood crib was thus added to the HRR of the first wood crib but starting at t =208 seconds. A comparison between the calculated HRR curve and the measured values of the test fire involving two wood cribs is shown in Figure 12:

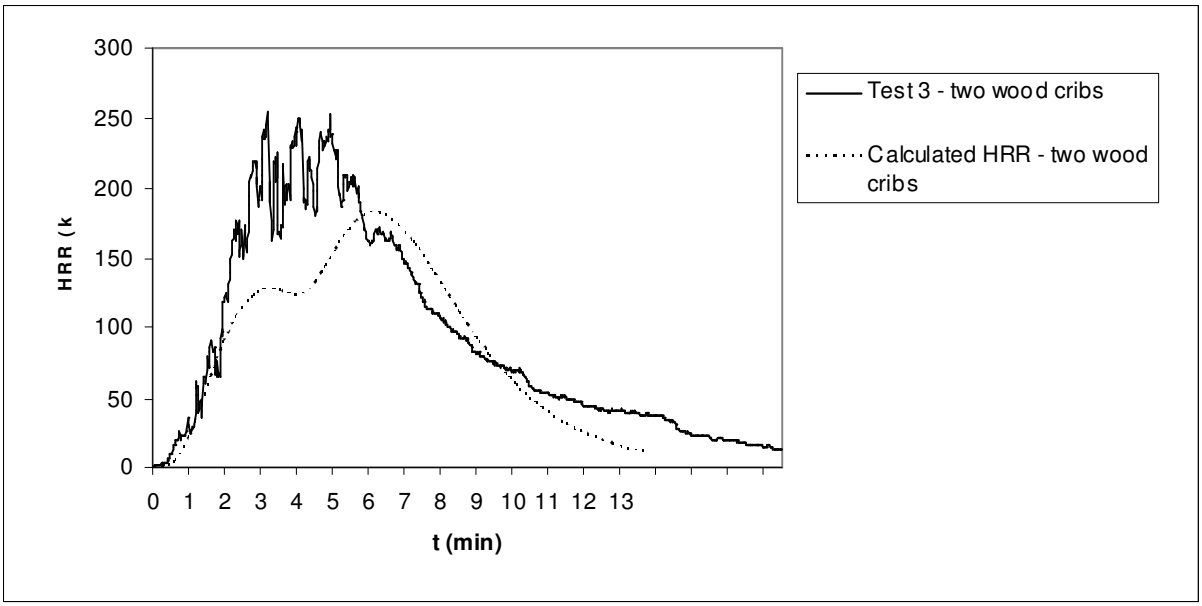

Figure 12. The HRR using the method with the ignition temperature as ignition criteria versus the measured HRR value.

As seen in Figure 12, the method does not agree as well with the measured values of test 3 (two wood cribs).

Using the same procedure as previously, a corner node temperature at the third wood crib could be calculated (the time is calculated from ignition of the first wood crib), see Figure 13

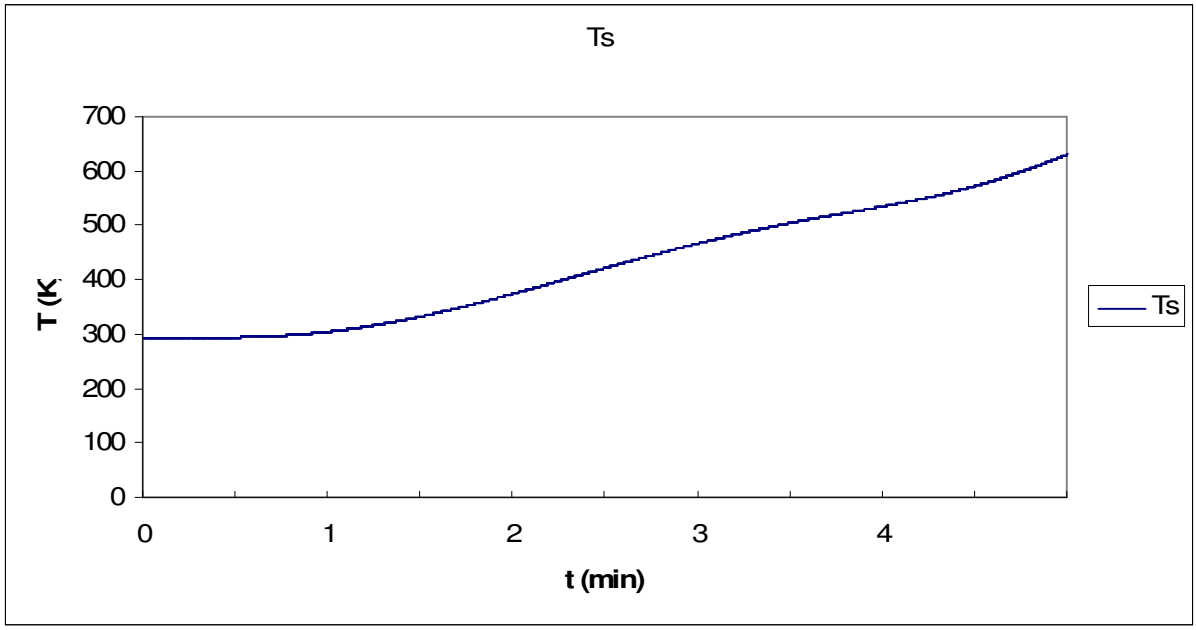

Figure 13. The corner node temperature at the third wood crib as a function of time.

The surface temperature was found to exceed the ignition temperature at 622 K after ~296 seconds at the corner nodes. The HRR of the third wood crib was thus added to the HRR of the first two wood cribs but starting at t=296 seconds.

A comparison between the calculated HRR curve and the measured values of the test fire involving three wood cribs is shown in Figure 14:

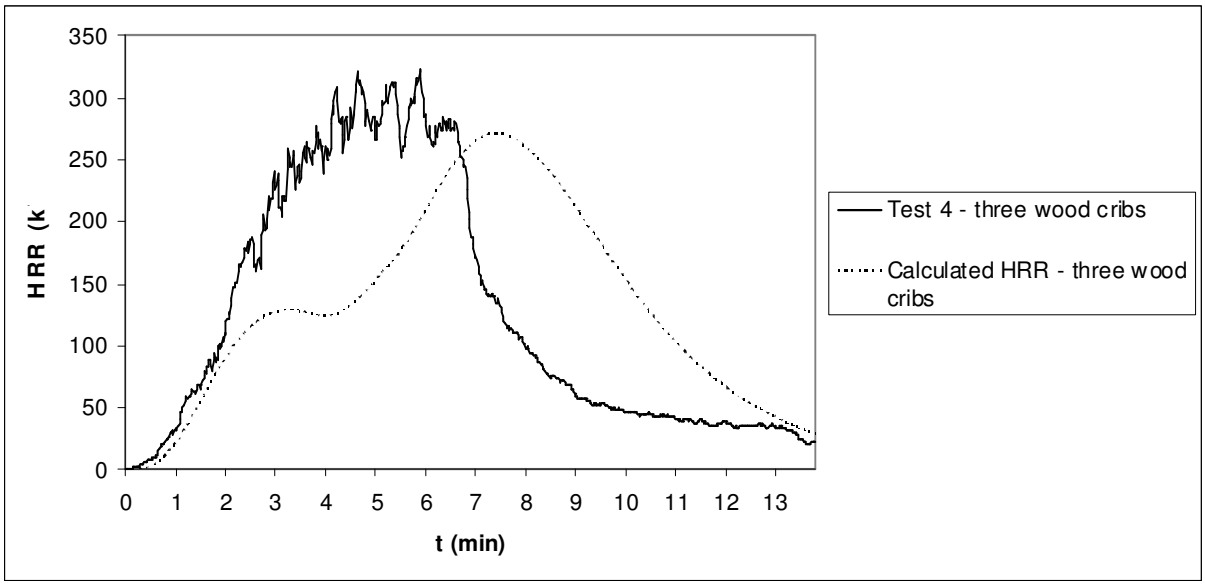

Figure 14. The HRR using the method with the ignition temperature as ignition criteria versus the measured HRR value.

As seen from Figure 14, the method does not agree very well with the measured values of test 4.

In order to further verify the results of the method, the total energy content of the calculated HRR curve and the energy content based upon the total mass of the involved wood cribs (i.e. the actual energy content) were compared, see Table 7. A conclusion with respect to the total energy content is that the energy content of the method matches well the actual energy content but the shape of the HRR is not satisfactory.

Table 7 Energy content calculated based on HRR curve or total mass.

Test #	Energy content based on HRR curve (MJ)	Energy content based on total mass (MJ)
3	74.0	74.1
4	109.6	113.4

In Babrauskas and Grayson [24] an algorithm is described that calculates the surface temperature of a thermally thick object accounting for a transient heat flux:

$$T_s(t) = T_\infty + \frac{1}{\sqrt{\pi \cdot k \cdot \rho \cdot c_p}} \int_0^t \frac{\dot{q}''_{net}(\tau)}{\sqrt{t-\tau}} d\tau \qquad (29)$$

Where:
$\dot{q}''_{net}$ is the net heat flux into the solid [kW/m²]

The algorithm contains an Abel integral which was evaluated numerically using the incident heat flux, $\dot{q}''_{flux}$, instead of the net heat flux, resulting in the following graph of the surface temperature at the second wood crib, see Figure 15.

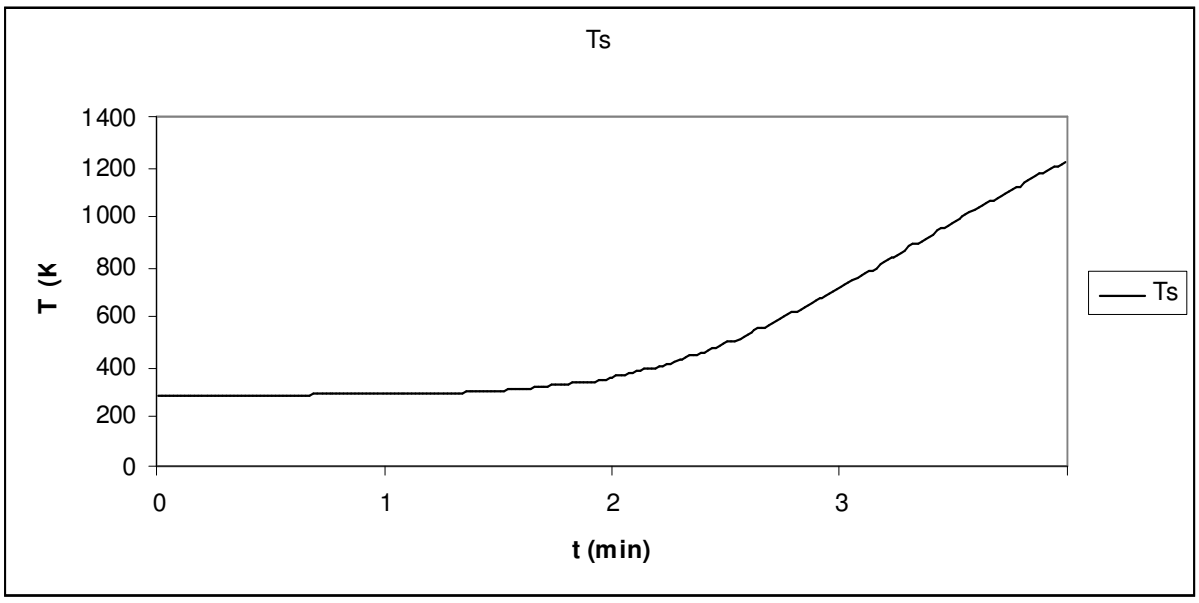

Figure 15. The surface temperature at the second wood crib using an algorithm containing an Abel integral.

The surface temperature was found to exceed the ignition temperature at 622 K after ~169 seconds. The HRR of the second wood crib was added to the HRR of the first wood crib but starting at $t = 169$ seconds. A comparison between the calculated HRR curve and the measured values of the test fire involving two wood cribs is shown in Figure 16:

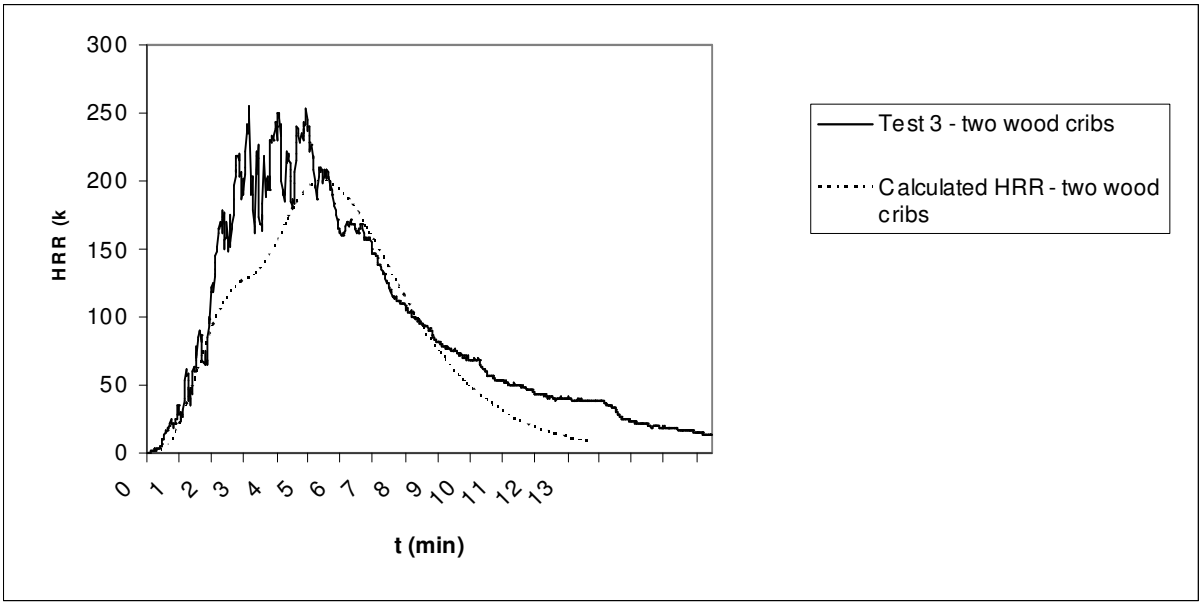

Figure 16. The HRR using the method with the ignition temperature as ignition criteria versus the measured HRR value.

As seen in Figure 16, the method does not agree well with the measured values of test 3.

Using the same procedure as previously, the following surface temperature at the third wood crib can be calculated, see Figure 17.

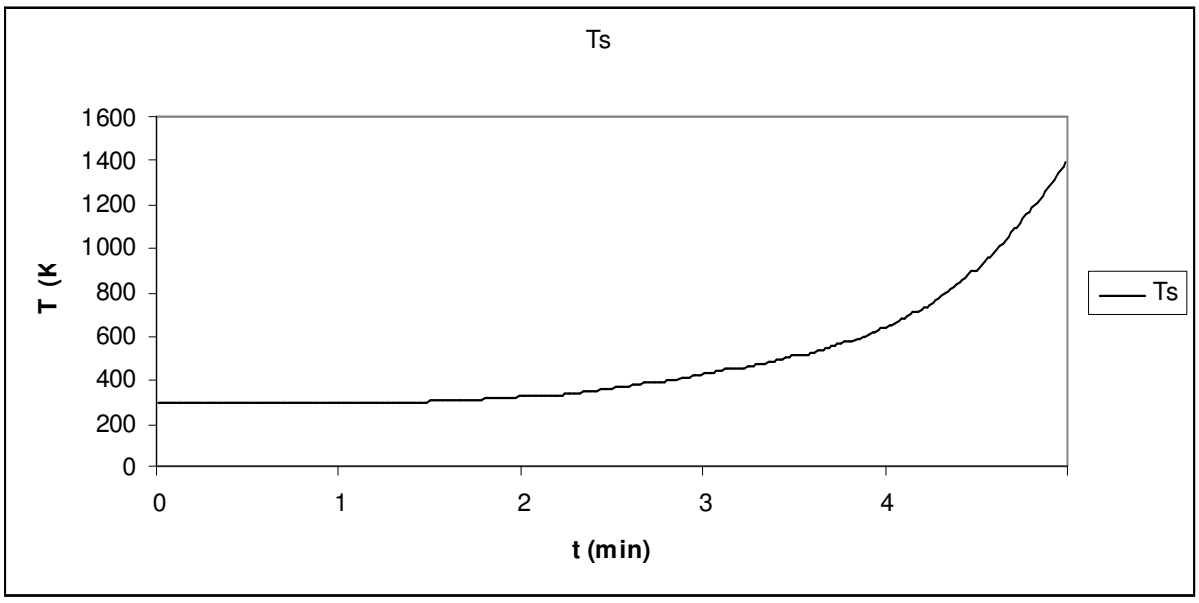

Figure 17. The surface temperature at the third wood crib using an algorithm containing an Abel integral.

The surface temperature was found to exceed the ignition temperature at 622 K after ~238 seconds. The HRR of the third wood crib was thus added to the HRR of the first and second wood crib but starting at t=238 seconds.

A comparison between the calculated HRR curve and the measured values of the test fire involving three wood cribs is shown in Figure 18.

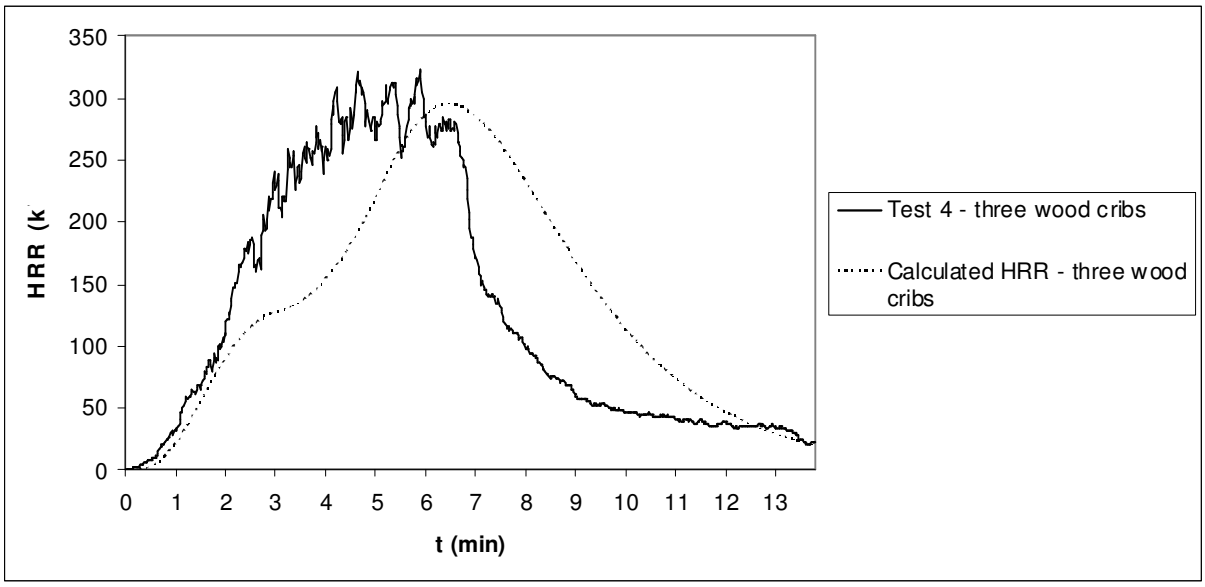

Figure 18. The HRR using the method with the ignition temperature as ignition criteria versus the measured HRR value.

As seen in Figure 18, the method does not agree well with the measured values of test 4.

In order to further verify the results of the method, the total energy content of the calculated HRR curve and the energy content based upon the total mass of the involved wood cribs (i.e. the actual energy content) were compared, see Table 8. One conclusion with respect to the

total energy content is that the energy content of the method matches well the actual energy content but poor prediction of the ignition time of the secondary objects makes the shape of the HRR not satisfactory. The reason why the total energy content matches well is because the energy balance is maintained through simple summation of individual HRR curves.

Table 8 Energy content calculated based on HRR curve or total mass.

Test #	Energy content based on HRR curve (MJ)	Energy content based on total mass (MJ)
3	74.4	74.1
4	110.7	113.4

A comparison between the total heat release curves of the three methods and the experimental data using three wood cribs is shown in Figure 19.

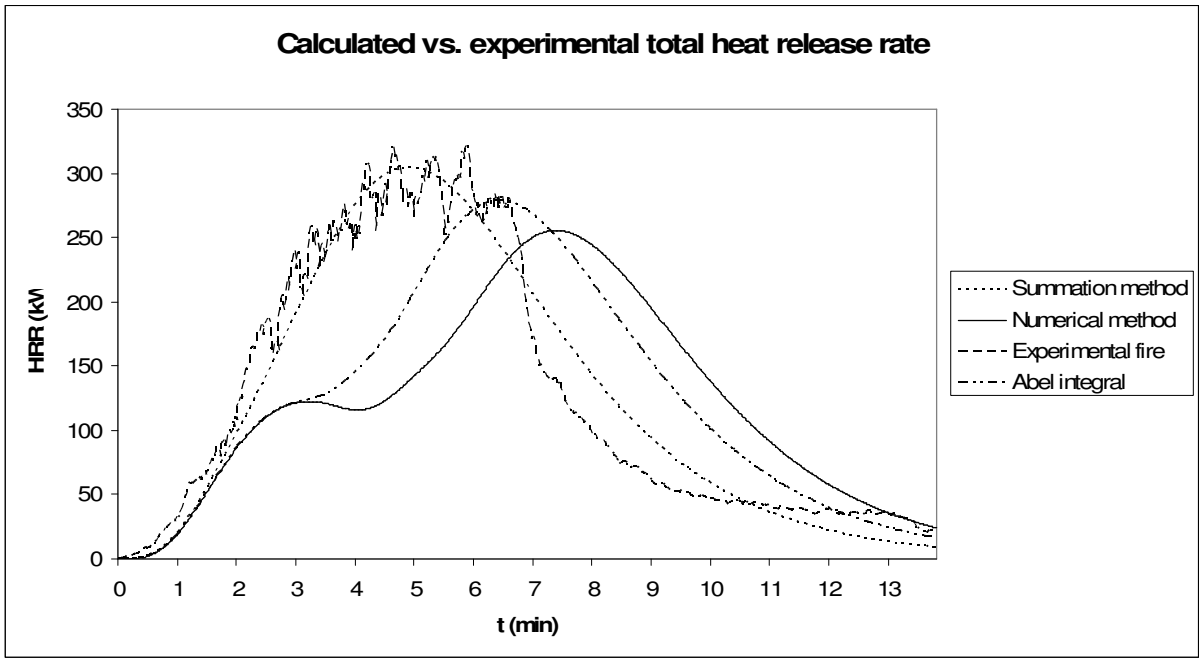

Figure 19. The calculated total HRR curve of the summation method and the two methods using the ignition temperature as critical value.

When comparing the graphs it is noted that the two methods do not agree well with the experimental data. The two methods predict a much later ignition of the adjacent wood cribs than seen from the experimental data.

Discussion

The results of the method using the critical heat flux as ignition criteria that was presented here, i.e. designing a HRR curve for multiple objects, agreed very well with the measured values of the corresponding test fires as well as comparing the calculated energy contents. This is a very promising result that can be used in future studies with respect to fires in tunnels, underground mines or other building constructions. One reason why the results of the method agreed very well with measured values could be that the ignition took place at an early stage and therefore the amount of heat accumulated in the wood crib was relatively low.

The results of the two methods using the ignition temperature as ignition criteria did not agree very well with the measured values of the corresponding tests 3 and 4. Most likely these methods were not suitable for this specific test case. A reason for this could be that the method responds too slowly to a rapid increase in fire gas temperature. Another reason could be that the ignition temperature is not a consistent value, but varies depending upon for example the heat flux, Tewarson [21]. The geometrical construction of the wood cribs may also play an important role for the heating process. Thus a case with a transient heat flux is not suited for a constant ignition temperature as an ignition criterion.

A prerequisite when working on the alternative methods was the fact that they should be kept relatively simple to be of practical use as engineering tools. When actually applying the three methods, the algorithm is fairly simple and a simple spreadsheet was used to simplify the calculations. The three methods could be considered as potential practical engineering tools.

Even though the items used in the fire tests and the calculations in this article are identical, the methods allow the calculation of the overall HRR of a truckload consisting of numerous types of cargo items, various distances etc. The only prerequisite is *a priori* knowledge of the HRR rate and energy content of each individual object. Finally, the prerequisite that the objects do not necessarily have to be of uniform composition is therefore fulfilled.

Conclusions

Theoretical calculations of the HRR of fire load consisting of different objects have been carried out and compared with the results from fire experiments using wood cribs. The results of the calculations can be summarised as follows:

- Three methods were presented that uses physical relationships. The first method uses a critical external heat flux as ignition criteria and the other two methods use a surface temperature as ignition criteria.
- The method using the critical heat flux as ignition criteria exhibited very good agreement with the corresponding results of performed fire experiments. This clearly shows the feasibility of the method for the problem when constructing an overall heat release curve for equally separated wood cribs in longitudinal flow in a tunnel configuration.
- The methods using the ignition temperature as ignition criteria did not agree very well with the corresponding results of performed fire experiments. Most likely these methods were not suitable for this specific case due to the fact that ignition of the adjacent wood cribs took place early and therefore the amount of energy accumulated in the wood cribs was limited. The geometrical construction of the wood cribs may also play a role for the heating process. Therefore the idea of using a constant ignition temperature as the ignition criteria for a case with a transient heat flux is not ideal
- All the prerequisites that were set up were fulfilled: the methods were kept relatively simple to be of practical use, and the cargo does not necessarily have to be of uniform composition. When using the three methods, the objects (e.g. cargo in a HGV) can very well consist of numerous types of objects, various distances etc.
- In order to further validate the three methods, the following work is recommended: the methods presented should be compared to more fire experiments; they should be applied to further non-uniform conditions, increasing the degree of realism; they should be applied to fires showing slower growth. Finally, a fire experiment with a mining vehicle in an underground mine should be performed and compared with the calculated values of the three presented methods. During the calculations the ignition

times of the various flammable objects on the vehicle – such as tyres, hoses, flammable liquid etc – should be calculated and a total heat release rate curve of the vehicle presented.

Acknowledgement

The project was sponsored by the Swedish Knowledge Foundation (KK-stiftelsen) and LKAB Mining Corporation.

References

[1] Numajiri F., and Furukawa K. (1998), *Short Communication: Mathematical Expression of Heat Release Rate Curve and Proposal of 'Burning Index',* Fire and Materials, vol 22, pp 39-42

[2] Ingason H. (2009), *Design fire curves for tunnels,* Fire Safety Journal, vol 44, pp 259-265

[3] Ingason H. (2005), *Fire Development in Large Tunnel Fires,* 8th Fire Safety Science Proceedings, pp 1497-1508

[4] Ingason H. (2005), *Model Scale Tunnel Fire Tests,* SP report 2005:49, Swedish National Testing and Research Institute

[5] Heskestad G., Modeling of Enclosure Fires, Proceedings of the Fourteenth Symposium (International) on Combustion, 1021-1030, The Pennsylvania State University, USA, August, 1972.

[6] Quintiere J. G., Scaling Applications in Fire Research, Fire Safety Journal, 15, 3-29, 1989.

[7] Heskestad G., Physical Modeling of Fire, Journal of Fire & Flammability, 6, 253-273, 1975.

[8] Heskestad G. Scaling the interaction of water sprays and flames, Fire Safety Journal, 2002, 37, 535-548.

[9] Heskestad G. Extinction of gas and liquid pool fires with water spray. 2003, 38, 301-317

[10] Yu H.Z., Zhou X.Y., Ditch B.D., Experimental validation of Froude-modeling-based physical scaling of water mist cooling of enclosure fires. Fire Safety Science-Proceedings of the ninth international sysposium, the International Assocation for Fire Safety Science, 2008, pp. 553-564.

[11] Ingason H., Li Y.Z., Model scale tunnel fire tests with longitudinal ventilation. Fire Safety Journal (Accepted).

[12] Li Y.Z., Lei B., and Ingason H., Study of critical velocity and backlayering length in longitudinally ventilated tunnel fires, Fire Safety Journal (Accepted).

[13] Ingason H., Li Y.Z., Model scale tunnel fire tests with extraction ventilation. Journal of Fire Protection Engineering, 2009 (submitted).

[14] Li Y.Z., Ingason H., Maximum temperature beneath ceiling in a tunnel fire. SP Report, 2010 :51.

[15] Ingason H., Li Y.Z., Model scale tunnel fire tests with extraction ventilation. SP Report 2010:03.

[16] Saito, N., Yamada, T., Sekizawa, A., Yanai, E., Watanabe, Y., and Miyazaki, S., "Experimental Study on Fire Behavior in a Wind Tunnel with a Reduced Scale Model", Second International Conference on Safety in Road and Rail Tunnels, 303-310, Granada, Spain, 3-6 April, 1995.

[17] Vantelon, J. P., Guelzim, A., Quach, D., Son, D., K., Gabay, D., and Dallest, D., "Investigation of Fire-Induced Smoke Movement in Tunnels and Stations: An Application to the Paris Metro", IAFSS Fire Safety Science-Proceedings of the third international symposium, pp. 907-918, Edinburg, 1991.

[18] Vauquelin, O. and Mégret, O., Smoke extraction experiments in case of fire in a tunnel. Fire Safety Journal, 2002, 37, 525-533.

[19] Vauquelin, O. and Telle, D., Definition and experimental evaluation of the smoke "confinement velocity" in tunnel fires. Fire Safety Journal, 2005. 40, 320-330.

[20] Wickström U., and Göransson U. (1992), *Full-scale/bench-scale correlations of wall and ceiling linings,* Fire and Materials, vol 16, pp 15-22

[21] The SFPE Handbook of Fire Protection Engineering, Third edition, 2002, NFPA, Quincy

[22] Babrauskas V. (2003), *Ignition Handbook*, Fire Science Publishers, Issaquah

[23] Holman J.P. (1992), *Heat Transfer,* Seventh edition, McGraw-Hill, Singapore

[24] Babrauskas V. and Grayson S.J. eds. (1992), *Heat Release in Fires,* Chapman and Hall, London